Study of scalar gradient fields by geometric measure theory

Jörg Schumacher

Fachbereich Physik, Philipps-Universität, D-35032 Marburg, Germany

(February 8, 2008)

Upper bounds of the Hausdorff volume of scalar gradient field graphs are derived by means of geometric measure theory. The approach reproduces that scalar gradient fields along a mean imposed scalar gradient become space filling for sufficiently high values of Schmidt numbers Sc. The bounds are consistent with findings from recent high-resolution numerical experiments for $1 \leq Sc \leq 64$, but too rough when compared with numerical simulations. A Reynolds number dependence of the bounds is found due to the additional scalar gradient stretching term in the equation of motion.
PACS: 47.27.Eq, 47.53.+n, 02.40.-k

Recent direct numerical simulations (DNS) suggested that the passive scalar mixing in a turbulent flow becomes more isotropic when the Schmidt number, $Sc = \nu/\kappa$, is increased to values larger than unity, but the Taylor Reynolds number, R_λ, of the advecting turbulent flow is kept constant [1,2]. Here ν is the kinematic viscosity of the fluid and κ the diffusivity of the passive scalar field $\theta(\mathbf{x}, t)$. The scalar was driven by a mean scalar gradient, $\mathbf{G} = G\mathbf{e}_\alpha$, in both simulations which causes deviations from isotropy of the small-scale statistics. For increasing Sc, scalar filaments can be advected to ever finer scales which steepens up the local gradients, $g_i = \partial_i \theta$. Large gradients (or fronts) that are aligned with the mean, i.e. g_α, occur already for $Sc \sim 1$ or even below and are associated with characteristic scalar structures, so-called ramps and cliffs (for further references, see [3]). A return to isotropic mixing is then thought as a growing compensation of those pronounced positive fronts by an increasing number of steep negative gradients with increasing Sc. Consequently, the probability density function of g_α gets more symmetric tails and odd order derivative moments decay.

Our understanding of this process for advection in Navier-Stokes flows is still incomplete and an investigation of geometric properties of scalar gradient fields was started therefore recently [4]. Fractal and multifractal properties of scalar gradient level sets and related quantities were studied there in a series of high-resolution DNS where, e.g., a higher degree of local isotropy was found to be related to a flater spectrum of generalized (multifractal) dimensions.

On the theoretical side, concepts of geometric measure theory [5] were used sucessfully for scalars in turbulence [6,7] and relations to the scaling behavior of low-order structure functions were established. An extension of the framework discussed the dependence of the geometric properties of scalar level sets on Schmidt (or Prandtl) number and on spatial separation scales, respectively [8]. The purpose of the present brief report is to step in at this point and to extend the approach to scalar gradient fields. We will focus on the physics in the Batchelor regime of scalar turbulence where the advecting flow is in its viscous subrange [9]. Scales below the Kolmogorov dissipation scale of fluid turbulence, $\eta = (\nu^3/\epsilon)^{1/4}$, but larger than the Batchelor scale $\eta_B = \eta/Sc^{1/2}$ are considered. ϵ is the energy dissipation rate of the flow. We will derive an upper bound for the scaling dimension of the Hausdorff volume of the scalar gradient field graph. This can give us an idea of how the gradients are distributed spatially and how this distribution depends on Sc. Our findings will be compared finally with high resolution numerical data for Schmidt numbers between 1 and 64 to test the sensitivity of the derived scaling dimension bounds.

The geometric measure theory generalizes concepts of differential geometry to non-smooth hypersurfaces embedded in an Euclidian space. The central object is the graph of the field under consideration, which is defined as

$$\Gamma_r = \{(\mathbf{x}, g_\alpha) | \mathbf{x} \in B_r \subset \mathrm{R}^3, \, g_\alpha = g_\alpha(\mathbf{x})\} . \tag{1}$$

In case of a smooth field this is a three-dimensional hypersurface embedded in four-dimensional space. In Fig. 1 such graph is shown over a two-dimensional plane that is vertical to the direction of $\mathbf{G}$. We observe that the hypersurface is strongly folded and rough for larger scales thus suggesting fractal properties.

The Hausdorff dimension of such a graph, D_H, (or more precisely the box counting dimension) is obtained from the scaling behavior of its Hausdorff volume $H(\Gamma_r)$ with respect to scale r, the radius of balls B_r of the covering [5,10],

$$H(\Gamma_r) = \int_{B_r} \sqrt{1 + r^2 |\nabla \tilde{g}_\alpha|^2} \, \mathrm{d}^3 \mathbf{x} \sim r^{D_H} . \tag{2}$$

The relative Hausdorff volume $H(\Gamma_r)/V_r$ can be estimated as

$$\frac{H(\Gamma_r)}{V_r} \leq \sqrt{1 + \frac{3}{4\pi r} \int_{B_r} |\nabla \tilde{g}_\alpha|^2 \, \mathrm{d}^3 \mathbf{x}} , \tag{3}$$

where the Cauchy-Schwartz inequality was used and $V_r = 4\pi r^3/3$. The scalar gradient field $g_\alpha(\mathbf{x}, t)$ is measured in units of its root mean square (rms) value, i.e. $\tilde{g}_\alpha = g_\alpha/\sqrt{\langle g_\alpha^2 \rangle_V}$. Here $V = L^3$ where L is the outer scale of turbulence. Similarly, $\tilde{G} = G/\sqrt{\langle g_\alpha^2 \rangle_V}$.

Progress is made now with a substitution of the gradient term in (3) by means of the advection-diffusion equation for the scalar gradient component,

$$\left[\partial_t + u_i \partial_i - \kappa \partial_i^2 \right] \tilde{g}_\alpha + (\partial_\alpha u_i) \tilde{g}_i = -\partial_\alpha u_\alpha \tilde{G}. \tag{4}$$

From the resulting second order balance one gets

$$|\nabla \tilde{g}_\alpha|^2 = \frac{1}{2\kappa} [(-u_i \partial_i + \kappa \partial_i^2) \tilde{g}_\alpha^2$$
$$- 2\tilde{g}_\alpha (\partial_\alpha u_i \tilde{g}_i + \partial_\alpha u_\alpha \tilde{G})], \tag{5}$$

where summation is carried out over index i only, but not over α. The time derivative is already omitted, because we will discuss the statistically stationary case. With substitution (5), inequality (3) becomes

$$\frac{H(\Gamma_r)}{V_r} \leq \sqrt{1 + \frac{3}{4\pi r \kappa} \int_{B_r} \left[(-u_i \partial_i + \kappa \partial_i^2) \frac{\tilde{g}_\alpha^2}{2} - \tilde{g}_\alpha (\partial_\alpha u_i) \tilde{g}_i - \tilde{g}_\alpha \partial_\alpha u_\alpha \tilde{G} \right] d^3\mathbf{x}}. \tag{6}$$

We will consider now the four integrals under the square root separately and denote them by I_1, I_2, I_3, and I_4. From (6), with incompressibility, and by applying the Gauss theorem, it follows for I_1

$$I_1 = \frac{3r}{2\kappa A_r} \oint_{\partial B_r} \tilde{g}_\alpha^2 (\mathbf{u} - \mathbf{u}_0) \cdot d\mathbf{A}. \tag{7}$$

$A_r = 4\pi r^2$ is the surface content of B_r and the surface normal vector points toward the origin of B_r. It is possible to add $\mathbf{u}_0 = \mathbf{u}(\mathbf{x}_0)$, the velocity at the center of B_r for which $\langle \mathbf{u}_0 \rangle_{\partial B_r} = 0$. At this point, it has to be assumed that the fluctuations $\tilde{g}_\alpha^2$ are equally distributed over the sphere ∂B_r in order to get $\oint \tilde{g}_\alpha^2 \mathbf{u}_0 \cdot d\mathbf{A} = 0$. The application of the Cauchy-Schwartz inequality results in

$$I_1 \leq \frac{3r}{2\kappa} \sqrt{\oint_{\partial B_r} \tilde{g}_\alpha^4 \frac{dA}{A_r}} \sqrt{\oint_{\partial B_r} ((\mathbf{u} - \mathbf{u}_0) \cdot \mathbf{n})^2 \frac{dA}{A_r}}. \tag{8}$$

The first square root is a scale resolved scalar gradient flatness which will be discussed later and denoted by $F_4(r) = \langle g_\alpha^4 \rangle_{B_r}/\langle g_\alpha^2 \rangle_V^2$. Note that the r-dependence comes in via coarse graining over balls of varying radius r. The second term stands for the second order longitudinal velocity structure function, which is $S_\parallel(r) = \epsilon r^2/(15\nu)$ in the viscous range, i.e. on scales around and below the Kolmogorov dissipation scale η. We find

$$I_1 \leq \frac{3}{2\kappa} \sqrt{\frac{\epsilon F_4(r)}{15\nu}} r^2. \tag{9}$$

Integral I_2 in (6) can be written as

$$I_2 = \frac{3}{4\pi r} \int_{B_r} \left[\tilde{g}_\alpha \nabla^2 \tilde{g}_\alpha + |\nabla \tilde{g}_\alpha|^2 \right] d^3\mathbf{x}. \tag{10}$$

Green's formula for scalars $u(\mathbf{x})$ and $v(\mathbf{x})$,

$$\int_V u(\mathbf{x}) \nabla^2 v(\mathbf{x}) d^3\mathbf{x} = \oint_{\partial V} u(\mathbf{x}) \nabla v(\mathbf{x}) \cdot d\mathbf{A}$$
$$- \int_V \nabla u(\mathbf{x}) \cdot \nabla v(\mathbf{x}) d^3\mathbf{x}, \tag{11}$$

with $u(\mathbf{x}) = v(\mathbf{x}) = \tilde{g}_\alpha(\mathbf{x})$ is taken. Substitution into (10) and application of the Cauchy-Schwartz inequality result in

$$I_2 = \frac{3}{4\pi r} \oint_{\partial B_r} \tilde{g}_\alpha |\nabla \tilde{g}_\alpha| \, \mathbf{n} \cdot d\mathbf{A}$$
$$\leq 3r \sqrt{\frac{1}{A_r} \oint_{\partial B_r} \tilde{g}_\alpha^2 \, dA} \sqrt{\frac{1}{A_r} \oint_{\partial B_r} |\nabla \tilde{g}_\alpha|^2 \, dA}$$
$$= 3r \sqrt{F_2(r)} \sqrt{\langle |\nabla \tilde{g}_\alpha|^2 \rangle_{\partial B_r}}, \tag{12}$$

with $F_2(r) = \langle g_\alpha^2 \rangle_{\partial B_r} / \langle g_\alpha^2 \rangle_V$ and $\nabla \tilde{g}_\alpha = |\nabla \tilde{g}_\alpha| \, \mathbf{n}$. We assume that the volume average as well as the surface average give the same results over scales r due to homogeneity of turbulence.

The third integral, I_3, can be estimated by the Cauchy-Schwartz inequality to

$$I_3 = -\frac{3}{4\pi r \kappa} \int_{B_r} \tilde{g}_\alpha (\partial_\alpha u_i) \tilde{g}_i \, \mathrm{d}^3 \mathbf{x}$$

$$\leq \frac{r^2}{\kappa} \sum_{i=1}^{3} \sqrt{\langle \tilde{g}_\alpha^2 \tilde{g}_i^2 \rangle_{B_r} \langle (\partial_\alpha u_i)^2 \rangle_{B_r}} \, . \tag{13}$$

It is reasonable to assume that the fluctuations along the mean scalar gradient are the largest so that the mixed terms can be estimated by $\langle \tilde{g}_\alpha^2 \tilde{g}_i^2 \rangle_{B_r} \leq \langle \tilde{g}_\alpha^4 \rangle_{B_r} = F_4(r)$ for $i \neq \alpha$. The velocity gradient can be treated by the energy dissipation averaged over balls B_r. Here we estimated $\sum_{i=1}^{3} \langle (\partial_\alpha u_i)^2 \rangle_{B_r} \leq \langle \epsilon \rangle_{B_r} / \nu$. The notation $\epsilon_r = \langle \epsilon \rangle_{B_r}$ is used for the following and consequently

$$I_3 \leq \frac{r^2}{\kappa} \sqrt{\frac{F_4(r) \epsilon_r}{\nu}} \, . \tag{14}$$

Similarily one can proceed for the integral I_4

$$I_4 = -\frac{3}{4\pi r \kappa} \int_{B_r} \tilde{g}_\alpha (\partial_\alpha u_\alpha) \tilde{G} \, \mathrm{d}^3 \mathbf{x} \leq \frac{r^2 \tilde{G}}{\kappa} \sqrt{\frac{F_2(r) \epsilon_r}{\nu}} \, . \tag{15}$$

In summary we get

$$\frac{H(\Gamma_r)}{V_r} \leq \sqrt{1 + \frac{3r^2}{2\kappa} \sqrt{\frac{\epsilon F_4(r)}{15\nu}} + 3r \sqrt{F_2(r) \langle |\nabla \tilde{g}_\alpha|^2 \rangle_{\partial B_r}} + \frac{r^2}{\kappa} \sqrt{\frac{F_4(r) \epsilon_r}{\nu}} + \frac{r^2 \tilde{G}}{\kappa} \sqrt{\frac{F_2(r) \epsilon_r}{\nu}}} \, . \tag{16}$$

Unfortunately left with a couple of unknown terms in this expression. Further progress can be made only by the use of dimensional arguments. One can expect that the energy dissipation field fluctuates most strongly around scale η and large velocity gradients will be smoothed by the finite viscosity on scales below. Therefore it is reasonable to assume

$$\frac{\epsilon_r}{\epsilon} \leq \frac{\epsilon_\eta}{\epsilon} \simeq \left(\frac{\eta}{L} \right)^{\gamma - 1} = \left(\frac{20}{3} R_\lambda^{-2} \right)^{\frac{3}{4}(\gamma - 1)} \, , \tag{17}$$

where $(\eta/L) = (20/3)^{3/4} R_\lambda^{-3/2}$ [11]. γ is a (universal) scaling exponent varying between γ_1 and γ_2. Clearly, the minimum exponent, γ_1, will be the dominant one.

The following term in I_2, can be simplified to

$$\langle |\nabla \tilde{g}_\alpha|^2 \rangle_{\partial B_r} \leq \frac{1}{\eta_B^2} \langle (\tilde{g}_\alpha)^2 \rangle_{\partial B_r} = \frac{F_2(r)}{\eta_B^2} \, , \tag{18}$$

and $F_2(r)$ follows in lines with (17) to

$$F_2(r) = \frac{\langle g_\alpha^2 \rangle_{\partial B_r}}{\langle g_\alpha^2 \rangle_V} \simeq \frac{\epsilon_{\theta,r}}{\epsilon_\theta} \leq \frac{\epsilon_{\theta,\eta_B}}{\epsilon_\theta} \simeq \left(\frac{\eta_B}{L} \right)^{\delta - 1} \, , \tag{19}$$

where $\epsilon_{\theta,r} = \langle \epsilon_\theta \rangle_{\partial B_r}$ is the coarse grained scalar dissipation rate. With $\eta_B / \eta = Sc^{-1/2}$ one gets

$$F_2(r) \leq \left[\left(\frac{20}{3} \right)^{\frac{3}{4}} Sc^{-\frac{1}{2}} R_\lambda^{-\frac{3}{2}} \right]^{\delta - 1} \, . \tag{20}$$

Again the scaling exponent $\delta \in [\delta_1, \delta_2]$. $F_4(r)$ can be estimated as follows

$$F_4(r) = \frac{\langle g_\alpha^4 \rangle_{B_r}}{\langle g_\alpha^2 \rangle_V^2} = \frac{\langle g_\alpha^4 \rangle_{B_r}}{\langle g_\alpha^4 \rangle_V} F_4(L) \leq \left(\frac{L}{\eta_B} \right)^4 F_4(L) \tag{21}$$

3

where $F_4(L) = \langle g_\alpha^4 \rangle_V / \langle g_\alpha^2 \rangle_V^2$, $\langle g_\alpha^4 \rangle_{B_r} \le G^4/\eta_B^4$, and $\langle g_\alpha^4 \rangle_V \simeq G^4/L^4$. G is the magnitude of the mean scalar gradient. It is also assumed that scalar gradient moments are at maximum around the Batchelor scale. Thus follows

$$F_4(r) \le \frac{27}{8000} Sc^2 R_\lambda^6 F_4(L). \tag{22}$$

The term I_3 will be much larger than I_4 if for the mean scalar gradient holds, $\tilde{G} \ll \sqrt{F_4(r)/F_2(r)}$, as it will be the case for the comparison with numerical experiments. Finally, I_1 will always be subdominant compared to I_3 due to $\epsilon_r \gg \epsilon$.

All the estimates are inserted now into (16) and we assume a scaling relation for the relative Hausdorff volume, $H(\Gamma_r)/V_r \sim r^{D_H-3}$. Additionally, all scales are expressed in units of Kolmogorov dissipation length, $\tilde{r} = r/\eta$. The Hausdorff dimension of the graph over two-dimensional balls is given by the additive law, $D_H' = D_H - 1$, [12] when assuming almost isotropic graphs,

$$D_H' = 2 + \frac{\mathrm{d} \ln(H(\Gamma_{\tilde{r}})/V_{\tilde{r}})}{\mathrm{d} \ln \tilde{r}}$$

$$\le 2 + \frac{\mathrm{d}}{\mathrm{d} \ln \tilde{r}} \ln \sqrt{1 + 3 \left[\left(\frac{20}{3}\right)^{\frac{3}{4}} R_\lambda^{-\frac{3}{2}} \right]^{\delta_1 - 1} Sc^{\frac{2-\delta_1}{2}} \tilde{r} + \sqrt{\frac{27 F_4(L)}{8000}} \left(\frac{20}{3}\right)^{\frac{3}{8}(\gamma_1-1)} Sc^2 R_\lambda^{\frac{15-3\gamma_1}{4}} \tilde{r}^2}. \tag{23}$$

The expression probes the local slope of the scaling relation. The upper bound of D_H' will be determined by the leading term under the square root at every scale $\tilde{r}$ and we expect the result $2 \le D_H' \le 3$.

The missing scalar derivative flatness factor $F_4(L)$ can be evaluated from [1] and present simulations. The latter are conducted in a homogeneously sheared flow in which the scalar field of constant gradient was allowed to evolve according to the advection-diffusion equation [4,13]. The mean scalar gradient is kept the same in all runs resulting in dimensionless $\tilde{G} = 0.37$ at $Sc = 1$ and 0.05 at $Sc = 64$ so that $\tilde{G} \ll \sqrt{F_4(r)/F_2(r)}$ is justified. As the inset of Fig. 2 shows, the flatness factors for both simulations are ~ 10 for $Sc > 1$ and will be taken constant for the following.

The two minimum scaling exponents, γ_1 and δ_1, can be taken from experiments where the whole multifractal spectrum for $\epsilon_\theta(\mathbf{x}, t)$ and $\epsilon(\mathbf{x}, t)$ was measured, respectively. Meneveau and Sreenivasan [14] found for experimental data at different Reynolds numbers that γ_1 is about 1/4. Prasad *et al.* found a value of $\delta_1 \approx 2/5$ in a high-Schmidt number scalar mixing experiment at $Sc \approx 2000$ [15].

Figure 2 plots (23) for three different values of Sc. For scales accessible to the simulations, i.e, larger than η_B the upper bound is found to be always 3. While for the scalar case the crossover of D_H' from 2 to 3 takes place around η_B [8], it is present here for by far smaller scales. It is just the fairly rough estimate for the additional scalar gradient stretching term (last term on the l.h.s. of (4)) that causes the crossover scale, $\tilde{r}_c$, to be smaller than η_B. When inserting the numbers, one gets $\tilde{r}_c \sim Sc^{-6/5} R_\lambda^{-213/80}$, at which the second term of (23) starts to dominate. To illustrate this effect, we kept I_1 only and plot the corresponding D_H' as dashed lines in Fig. 2. The bounds are shifted then by an order of magnitude, but still rough due to estimate (22).

For comparison, we conducted the relative Hausdorff volume of the scalar gradient field from numerical simulation data. Two-dimensional "balls" are then squares of a dyadic grid of sidelength $2^{-j} \times 2\pi$. The corresponding local slope of the scaling dimension is added in Fig. 2 and a plateau with a non-integer dimension of $D_H' \approx 2.3$ can be observed for intermediate scales. This feature cannot be reproduced by the upper bounds because the $\tilde{r}$-dependence of all four I terms has integer powers only. Even for passive scalars, non-integer D_H were obtained only for inertial range scaling of the velocity structure function of $\sim r^{2/3}$ (cf. [8]).

To summarize, we have discussed the applicability of the geometric measure theory to scalar gradient fields for high-Sc mixing. The upper bounds on D_H are consistent with simulation results but rough. Additionally, they are insensitive to the particular choice of the threshold value of the level set and thus cannot capture slight differences between positive and negative level sets of same magnitude which were discussed in [4]. Interestingly, a dependence of the bounds on the Taylor-Reynolds number results. Batchelor's original model for the visocous-convective range was thought to be insensitive to the physics in the inertial range, i.e., on scales larger η [9]. A detailed investigation of that problem will be a part of future work and further improvement and extension of the bounds might be possible therefore.

[1] P. K. Yeung, S. Xu, and K. R. Sreenivasan, Phys. Fluids **14**, 4178 (2002).

[2] G. Brethouwer, J. C. R. Hunt, and F. T. M. Nieuwstadt, J. Fluid Mech. **474**, 193 (2003).

[3] Z. Warhaft, Annu. Rev. Fluid Mech. **32**, 203 (2000).

[4] J. Schumacher and K. R. Sreenivasan, Phys. Rev. Lett. **91**, 174501 (2003).

[5] F. Morgan, *Geometric Measure Theory, a Beginners Guide*, (Academic Press, Boston) 1988.

[6] P. Constantin, I. Procaccia, and K. R. Sreenivasan, Phys. Rev. Lett. **67**, 1739 (1991).

[7] P. Constantin and I. Procaccia, Phys. Rev. E **47**, 3307 (1993).

[8] S. Grossmann and D. Lohse, Europhys. Lett. **27**, 347 (1994); B. Eckhardt and J. Schumacher, Phys. Rev. E **60**, 4185 (1999).

[9] G. K. Batchelor, J. Fluid Mech. **5**, 113 (1959).

[10] K. J. Falconer, *The Geometry of Fractal Sets*, Cambridge University Press, Cambridge 1985.

[11] S. B. Pope, *Turbulent flows*, Cambridge University Press, Cambridge 2000.

[12] P. Mattila, Ann. Acad. Sci. Fenn. Ser. A. Math. **1**, 227 (1975).

[13] J. Schumacher and B. Eckhardt, Europhys. Lett. **52**, 627 (2000); J. Schumacher, J. Fluid Mech. **441**, 109 (2001).

[14] C. Meneveau and K. R. Sreenivasan, Phys. Rev. A **38**, 6287 (1989).

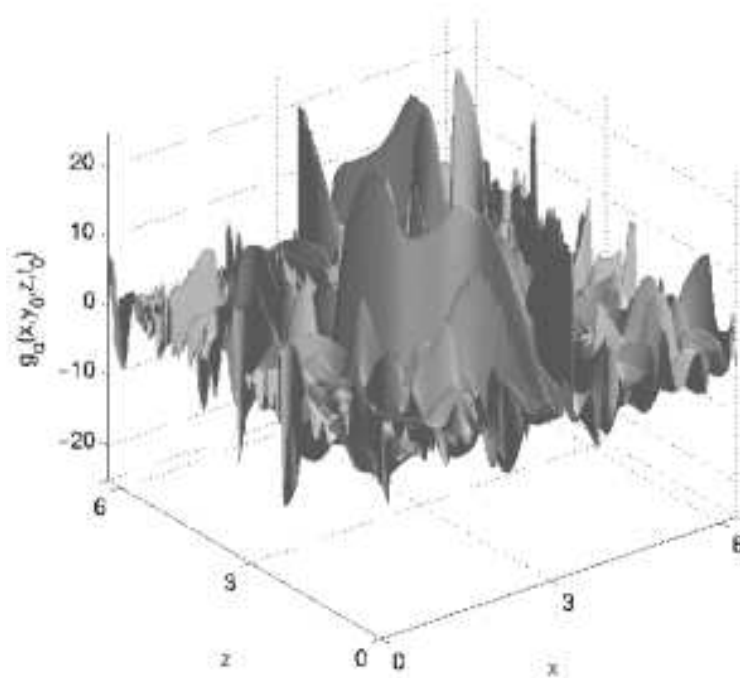[15] R. R. Prasad, C. Meneveau and K. R. Sreenivasan, Phys. Rev. Lett. **61**, 74 (1988).

FIG. 1. The graph of the scalar gradient field g_α which is shown here over the $x - z$ plane at fixed y_0 and t_0 for numerical data at $Sc = 16$. Grid resolution was $N = 512$.
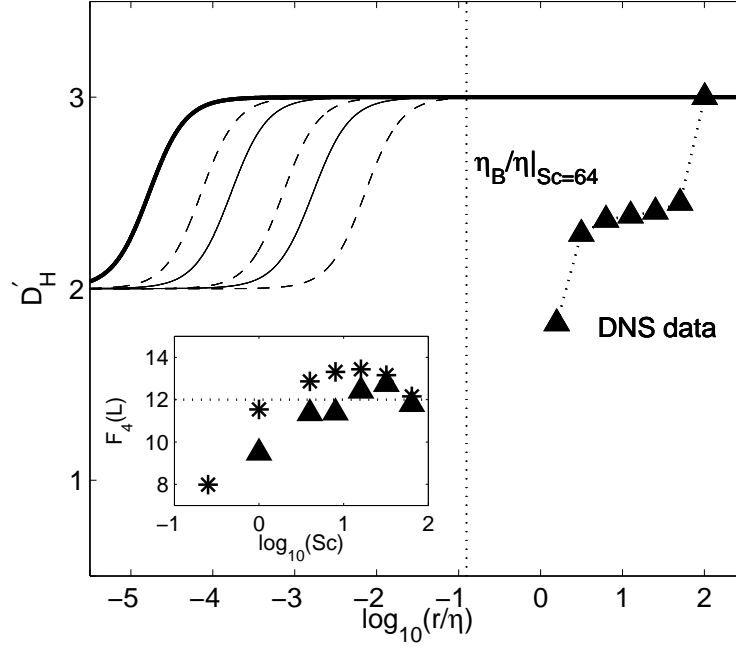
FIG. 2. Scale dependent upper bound of the Hausdorff dimension of scalar gradient level sets for different Schmidt numbers. Value of $R_\lambda = 87$ is taken from [4]. Solid lines are for $Sc = 64$ (thick line), 6.4, and 0.64 from left to right. Dashed lines are for bounds at the same Sc if integral I_1 would dominate in (23) as in the scalar case [8]. The Batchelor scale for $Sc = 64$ is marked as a dotted vertical line. The panel contains also the DNS findings for the scale resolved D'_H for $Sc = 64$ with a plateau at a value of about 2.3 . Inset: Flatness factor $F_4(L)$ of the scalar derivative along the mean scalar gradient, g_α, as a function of the Schmidt number. The dotted line stands for the mean of all data points and is drawn at 12. Present data are indicated by triangles and data from [1] by asterisks.